
ACCELERATING SPECTRAL CLUSTERING ON QUANTUM AND ANALOG PLATFORMS

Xingzi Xu *

Department of Electrical and Computer Engineering
Duke University
Durham, NC, USA
xingzi.xu@duke.edu

Tuhin Sahai

SRI International
Menlo Park, CA, USA
tuhin.sahai@sri.com

ABSTRACT

We introduce a novel hybrid quantum-analog algorithm to perform graph clustering that exploits connections between the evolution of dynamical systems on graphs and the underlying graph spectra. This approach constitutes a new class of algorithms that combine emerging quantum and analog platforms to accelerate computations. Our hybrid algorithm is equivalent to spectral clustering and has a computational complexity of $O(N)$, where N is the number of nodes in the graph, compared to $O(N^3)$ scaling on classical computing platforms. The proposed method employs the dynamic mode decomposition (DMD) framework on data generated by Schrödinger dynamics embedded into the manifold generated by the graph Laplacian. We prove and demonstrate that one can extract the eigenvalues and scaled eigenvectors of the normalized graph Laplacian from quantum evolution on the graph by using DMD computations.

1 Introduction

Graph clustering is a technique used to identify and group densely connected subgraphs within a larger graph. It is a powerful decomposition approach that enables the analysis of interconnected systems for a variety of applications in various fields, such as social networks [1, 2, 3], fraud detection [4, 5], bioinformatics [6], uncertainty analysis in networked systems [7], decomposition for scientific computation [8], and transport networks [9]. Consequently, the versatility of graph clustering makes it an invaluable tool in a wide range of areas ranging from scientific discovery to industrial applications. Spectral clustering, a specific graph decomposition approach, is particularly advantageous in high-dimensional spaces where the geometric characteristics of the data are not readily apparent [10]. Unlike traditional clustering methods, spectral clustering uses the properties of the eigenvalues and eigenvectors of the Laplacian of the underlying graph (or data) to find the optimal partitioning. This aspect enables spectral clustering to cluster points based on their interconnectedness rather than their raw distances from each other, typically resulting in better performance when dealing with data where the clusters are irregular, intertwined, or lie on a complex surface.

In this work, we propose a fast quantum-analog hybrid algorithm based on Schrödinger dynamics and dynamic mode decomposition (DMD) to rapidly retrieve accurate spectral clustering information. We evolve the underlying Schrödinger dynamics on quantum devices, and perform the subsequent spectrum computations on analog machines. The approach has a scaling of $O(N)$, where N is the number of nodes in the graph. Since existing state-of-the-art classical methods scale as $O(N^3)$, our approach provides a polynomial speed-up over traditional computing platforms. To the best of our knowledge, this is the first algorithm that exploits a combination of quantum and analog computing platforms to extract a scaling that is superior to algorithms that run on a single computing platform.

In quantum computing, qubits, the fundamental elements of quantum information, evolve according to the time-dependent Schrödinger's equation. Qubits differ from classical bits in that they can exist in a superposition of states, meaning that a qubit can be in states representing the traditional bits (0, 1) or a superposition of both. Quantum algorithms provide substantial reductions in computational complexity for specific problems such as integer factorization [11], database search [12], solving linear systems [13], and matrix multiplication [14] to name a few. Analog computing with

*Work performed as an intern in the Applied Sciences Lab at SRI International.

resistive memory has a fast response speed and embeds parallelism, significantly accelerating matrix computation [15]. Analog computing has garnered attention due to its potential to reduce the data movement bottleneck in traditional computing architectures. The essence of analog computing is performing computational operations directly at the data’s location rather than moving data between memory and the central processing unit (CPU). Integrating crosspoint arrays with negative feedback amplifiers allows for addressing linear algebra challenges like solving linear systems and determining matrix eigenvectors in a single step. Analog computing improves the exponential solving of linear systems and has a computational complexity of $\mathcal{O}(1)$ for matrix-vector multiplication [15, 16].

Despite the supreme performance of spectral clustering, it suffers from a time complexity of $\mathcal{O}(N^3)$, where N is the number of nodes, limiting its applications in large graphs [17]. We show that spectral clustering has an $\mathcal{O}(N)$ complexity on a hybrid algorithm employing quantum computers and analog computers.

We organize the rest of the paper as follows: Section 3.1 provides a brief overview of spectral clustering. Section 3.2 delves into the decentralized algorithm for spectral clustering, drawing on the wave equation and Dynamic Mode Decomposition (DMD). Quantum simulation of wave dynamics is covered in Section 3.3. Section 3.4 discusses singular value decomposition and eigendecomposition on an analog computer. How to solve a linear system for the eigenvectors using quantum or analog computers is detailed in Section 3.5. We round off with empirical findings in Section 4 and wrap up with conclusions in Section 5.

2 Analog matrix computing circuits

Conventional computers have significantly improved in speed and efficiency over the past decades, thanks to Moore’s law, which states that the number of transistors in an integrated circuit doubles about every two years [18]. However, the industry is approaching a limit where it is impossible to reduce the size of transistors [19]. In addition, due to the high computational complexity in conventional digital computers, the emerging need for scalable matrix-vector multiplication rooting from artificial intelligence further calls for different computing devices. With their abilities on matrix operations such as matrix multiplication, inversions, and pseudoinverse in one operation, analog matrix computing (AMC) circuits based on crosspoint resistive memory arrays provide an able alternative [15].

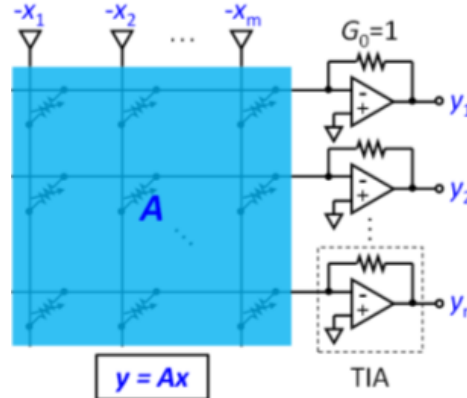


Figure 1: Schematic of AMC circuits for matrix-vector multiplication between positive matrix \mathbf{A} and vector \mathbf{x} [15].

For the multiplication between an $m \times n$ matrix and an $n \times 1$ vector, the computational complexity is $\mathcal{O}(mn)$ for digital computers and $\mathcal{O}(1)$ for AMC circuits [15]. The schematic of AMC circuits for computing the matrix-vector multiplication (MVM) between a positive matrix \mathbf{A} and a vector \mathbf{x} is in figure 1. The conductance of the circuits stores the values of \mathbf{A} , and the voltages applied on the circuit are the values of $-\mathbf{x}$, the output current values are the result $\mathbf{y} = \mathbf{A}\mathbf{x}$, by applying the Ohm’s law [20]. Since conductance can only be positive, matrices with negative entries split as $\mathbf{A} = \mathbf{A}_+ - \mathbf{A}_-$, where \mathbf{A}_+ is \mathbf{A}_- are both positive. The results are then calculated as $\mathbf{A}\mathbf{x} = \mathbf{A}_+\mathbf{x} - \mathbf{A}_-\mathbf{x}$. Unlike digital computers, analog computers compute the MVM results for all entries in parallel after setting the conductances and applying the voltages. To quantify the error and computational time of MVM on analog computers, we prove the following theorem using circuit dynamics.

Theorem 1. *Time for convergence (up to a tolerance of error ϵ between the computed and true solutions) of matrix-vector multiplication on circuit-based analog computers is bounded by,*

$$T = \max_j \frac{1}{\beta_j} \ln\left(\frac{x_0\beta - \alpha_j}{\epsilon}\right). \tag{1}$$

Proof. Given the evolution dynamics of analog circuits is given by [21],

$$\frac{dx(t)}{dt} = L_0\omega_0 U(Ay - x(t)), \quad (2)$$

where L_0 is the DC loop gain, ω_0 is the 3-dB bandwidth, y is an input vector, A is the conductance matrix, and

$$U = \mathbf{D} = \begin{pmatrix} \frac{1}{1+\sum_i A_{1i}} & 0 & \cdots & 0 \\ 0 & \frac{1}{1+\sum_i A_{2i}} & \cdots & 0 \\ \vdots & \vdots & \ddots & \vdots \\ 0 & 0 & \cdots & \frac{1}{1+\sum_i A_{ni}} \end{pmatrix}. \quad (3)$$

Expanding the above equations, it is easy to show that the j -th equation is given by,

$$\frac{dx_j(t)}{dt} = \alpha_j - \beta_j x_j(t), \quad (4)$$

where α_j and β are constants given by,

$$\begin{aligned} \alpha_j &= L_0\omega_0 \frac{\sum_i A_{ji}y_i}{1 + \sum_i A_{ji}}, \\ \beta_j &= \frac{L_0\omega_0}{1 + \sum_i A_{ji}}. \end{aligned} \quad (5)$$

Note that Eqns. 4 are all decoupled and their solution at time t is given by

$$x(t) = \frac{(x(0)\beta_j - \alpha_j)e^{-\beta_j t} + \alpha_j}{\beta_j}. \quad (6)$$

Now, let the solution as $t \rightarrow \infty$ is $x_f = \frac{\alpha_j}{\beta_j}$. If we now consider a time T_j such that the error $\|x(t) - x_f\|$ is less than equal to ϵ we get,

$$\frac{(x(0)\beta_j - \alpha_j)e^{-\beta_j t}}{\beta_j} \leq \epsilon, \quad (7)$$

or,

$$T_j \geq \frac{1}{\beta_j} \ln\left(\frac{x_0\beta - \alpha_j}{\epsilon}\right). \quad (8)$$

It now follows that the minimum time for convergence of the system (measured by the error reducing below a threshold of ϵ) is given by maximum over all j ,

$$T = \max_j \frac{1}{\beta_j} \ln\left(\frac{x_0\beta - \alpha_j}{\epsilon}\right). \quad (9)$$

□

3 Hybrid computation of spectral clustering

3.1 Spectral clustering

Consider a graph denoted $\mathcal{G} = (V, E)$ that consists of a vertex set $V = 1, \dots, N$ and an edge set $E \subseteq V \times V$. Each edge $(i, j) \in E$ in this graph is associated with a weight $\mathbf{W}_{ij} > 0$, and \mathbf{W} represents the $N \times N$ weighted adjacency matrix of \mathcal{G} . In this context, $\mathbf{W}_{ij} = 0$ only if $(i, j) \notin E$. The normalized graph Laplacian, represented by \mathbf{L} , is defined as follows:

$$\mathbf{L}_{ij} = \begin{cases} 1, & \text{if } i = j, \\ -\mathbf{W}_{ij} / \sum_{l=1}^N \mathbf{W}_{il}, & \text{if } (i, j) \in E, \\ 0, & \text{otherwise,} \end{cases} \quad (10)$$

An equivalent representation of the normalized graph Laplacian is $\mathbf{L} = \mathbf{I} - \mathbf{D}^{-1}\mathbf{W}$, where \mathbf{D} is a diagonal matrix that consists of the sums of the rows of \mathbf{W} . We focus solely on undirected graphs, for which the Laplacian is symmetric, and the eigenvalues are real numbers. The eigenvalues of \mathbf{L} can be arranged in ascending order as $0 = \lambda_1 \leq \lambda_2 \leq \dots \leq \lambda_N$. Each eigenvalue corresponds to an eigenvector, denoted as $\mathbf{v}^{(1)}, \mathbf{v}^{(2)}, \dots, \mathbf{v}^{(N)}$, where $\mathbf{v}^{(1)} = \mathbf{1} = [1, 1, \dots, 1]^T$ [10]. For our study, we assume $\lambda_1 < \lambda_2$, which means that the graph does not contain disconnected clusters. Spectral clustering partitions the graph \mathcal{G} into two clusters by employing the signs of the entries of the second eigenvector $\mathbf{v}^{(2)}$. Signs of entries of higher eigenvectors or k -means clustering can cluster nodes into more than two clusters [10]. Note that spectral gap heuristics can determine the cluster numbers.

3.2 Wave equation based clustering method

As in [22, 23], we consider the wave equation

$$\frac{\partial^2 u}{\partial t^2} = c^2 \Delta u. \quad (11)$$

The discretized wave equation on a graph is given by,

$$\mathbf{u}_i(t) = 2\mathbf{u}_i(t-1) - \mathbf{u}_i(t-2) - c^2 \sum_{j \in \mathcal{N}(i)} \mathbf{L}_{ij} \mathbf{u}_j(t-1), \quad (12)$$

where $\mathcal{N}(i)$ is the set of neighbors of node i including the node i itself [24]. To update \mathbf{u}_i , one only needs the previous value of \mathbf{u}_j at the neighboring nodes and the connecting edge weights.

Given the initial condition $\frac{d\mathbf{u}}{dt}(0) = 0$ and $0 < c < \sqrt{2}$, the solution of the wave equation 12 can be written as

$$\mathbf{u}(t) = \sum_{j=1}^N \mathbf{u}(0)^T \mathbf{v}^{(j)} (p_j e^{it\omega_j} + q_j e^{-it\omega_j}) \mathbf{v}^{(j)}, \quad (13)$$

where $p_j = (1 + i \tan(\omega_j/2))/2$, $q_j = (1 - i \tan(\omega_j/2))/2$ [23]. Now, finding the eigenvectors of \mathbf{L} is transformed into finding the coefficients of the wave dynamics in equation 13.

Dynamic Mode Decomposition (DMD) is a powerful tool for analyzing the dynamics of nonlinear systems and can be interpreted as an approximation of Koopman modes [25]. We apply DMD to one-dimensional time series data with time-delay embedding by constructing the matrix \mathbf{X} and \mathbf{Y} for the exact DMD matrix $\mathbf{A} = \mathbf{Y}\mathbf{X}^+$ (where $+$ denotes the pseudoinverse) [26]. When DMD with time delay embedding is implemented on one-dimensional signals of the structure

$$u(t) = \sum_{j=1}^J a_j e^{i\omega_j t}, \quad (14)$$

where $\omega_j \in (-\pi, \pi)$, $j = 1, 2, \dots, J$ are unique frequencies, it can successfully extract the coefficients a_j [23, 26].

We form the following matrices with the one-dimensional signal $u(t)$,

$$\mathbf{X} := \begin{bmatrix} u(0) & u(1) & \dots & u(M-1) \\ u(1) & u(2) & \dots & u(M) \\ \vdots & \vdots & \ddots & \vdots \\ u(K-1) & u(K) & \dots & u(K+M-2) \end{bmatrix} \quad (15)$$

$$= [\mathbf{x}^l(0) \quad \mathbf{x}^l(1) \quad \dots \quad \mathbf{x}^l(M-1)], \quad (16)$$

$$\mathbf{Y} := [\mathbf{x}^l(1) \quad \dots \quad \mathbf{x}^l(M-1) \quad \mathbf{x}^l(M)] \quad (17)$$

where $\mathbf{x}(t) := [u(t), u(t+1), \dots, u(t+(M-1))]^T$. Let $H > 1$, also define

$$\Phi_H := \begin{bmatrix} 1 & 1 & \dots & 1 \\ e^{i\omega_1} & e^{i\omega_2} & \dots & e^{i\omega_N} \\ \vdots & \vdots & \ddots & \vdots \\ e^{i(H-1)\omega_1} & e^{i(H-1)\omega_2} & \dots & e^{i(H-1)\omega_N} \end{bmatrix} \quad (18)$$

$$= [\phi_1, \phi_2, \dots, \phi_N], \quad (19)$$

where $\phi_j = [1, e^{i\omega_j}, \dots, e^{i(H-1)\omega_j}]^T$. [23] presented the following lemma

Lemma 1. For one-dimensional signal $u(t)$ defined by equation (14), if $K \geq J$ and $M \geq J$ of the matrices \mathbf{X} and \mathbf{Y} defined by (15) and (17) respectively, the eigenvalues of $\mathbf{A} = \mathbf{Y}\mathbf{X}^+$ are $\{e^{i\omega_j}\}_{j=1}^J$ and the columns of Φ_K defined by (18) are the corresponding eigenvectors [23].

Lemma 2. At node l , DMD on matrices $\mathbf{X}(u_l)$, $\mathbf{Y}(u_l)$ using local snapshots $\mathbf{u}_l(0), \mathbf{u}_l(1), \dots, \mathbf{u}_l(4N - 1)$ defined by 13 with $K = M = 2N$ yields exact eigenvalues of the Laplacian and the corresponding eigenvectors (scaled) [23].

Based on lemma 2, [23] developed a DMD based algorithm for distributed spectral clustering, given in algorithms 1, 2.

Algorithm 1 DMD(\mathbf{X}, \mathbf{Y}): For computing eigenvalues and eigenvector components at node i [23].

- 1: Compute reduced SVD of \mathbf{X} , i.e., $\mathbf{X} = \mathbf{U}\Sigma\mathbf{V}^*$.
 - 2: Define the matrix $\tilde{\mathbf{A}} \equiv \mathbf{U}^*\mathbf{Y}\mathbf{V}\Sigma^{-1}$
 - 3: Compute eigenvalues μ and eigenvectors ω of $\tilde{\mathbf{A}}$, i.e., $\tilde{\mathbf{A}}\omega = \mu\omega$. Each nonzero eigenvalue μ is a DMD eigenvalue.
 - 4: The DMD mode corresponding to μ is then given by $\hat{\phi} \equiv \frac{1}{\mu}\mathbf{Y}\mathbf{V}\Sigma^{-1}\omega$.
 - 5: Compute $\hat{\mathbf{a}}$ by solving the linear system $\hat{\Phi}\hat{\mathbf{a}} = \mathbf{x}(0)$, where the columns of $\hat{\Phi}$ are the eigenvectors sorted in decreasing order based on the real part of the eigenvalues.
 - 6: $a_i^{(j)} = \hat{\phi}_{j,1}\hat{a}_j, j = 1, 2, \dots, k$.
-

Algorithm 2 Wave equation based graph clustering [23].

- 1: $\mathbf{u}_i \leftarrow \text{Random}([0, 1])$
 - 2: $\mathbf{u}_i(-1) \leftarrow \mathbf{u}_i(0)$
 - 3: $t \leftarrow 1$
 - 4: **while** $\text{dot} < T_{\max}$
 - 5: $\mathbf{u}_i(t) \leftarrow 2\mathbf{u}_i(t-1) - \mathbf{u}_i(t-2) - c^2 \sum_{j \in \mathcal{N}(i)} \mathcal{L}_{ij}\mathbf{u}_j(t-1)$
 - 6: $t \leftarrow t + 1$
 - 7: **end while**
 - 8: Create the matrices $\mathbf{X}_i, \mathbf{Y}_i \in \mathbb{R}^{K \times M}$ defined by 15 and 17 at node i ,
 - 9: using $\mathbf{u}_i(0), \mathbf{u}_i(1), \dots, \mathbf{u}_i(T_{\max} - 1)$ where $K + M = T_{\max}$.
 - 10: $\mathbf{v}_i \leftarrow a_i$ from DMD($\mathbf{X}_i, \mathbf{Y}_i$) by algorithm 1
 - 11: **for** $j \in \{1, \dots, k\}$ **do**
 - 12: **if** $\mathbf{v}_i^{(j)} > 0$ **then**
 - 13: $A_j \leftarrow 1$
 - 14: **else**
 - 15: $A_j \leftarrow 0$
 - 16: **end if**
 - 17: **end for**
-

3.3 Simulation of wave dynamics

Conventional computers suffer from various computational challenges and inherent truncation errors in the simulation process when performing dynamics simulations. In particular, matrix multiplication, central to such simulations, has a computational complexity that goes up to $\mathcal{O}(N^{2.371866})$ on digital computers [27]. The algorithm with this complexity also has reduced numerical stability, compared to the naive $\mathcal{O}(N^3)$ algorithm [27]. On the contrary, quantum and analog computers demonstrate inherent prowess in this domain, boasting exponential speed advantages for simulating dynamical systems compared to their digital counterparts [28, 29, 30]. For our specific case of evolving wave dynamics, we can either simulate such dynamics continuously on a quantum computer or discretely on an analog device. At the same time, the continuous simulations on quantum computers avoid the truncation errors met in discrete simulations on analog or digital computers.

The wave equation on a graph is similar to equation 11, given as

$$\frac{d^2\mathbf{u}}{dt^2} = -c^2\mathbf{L}\mathbf{u} \quad (20)$$

where \mathbf{L} is the graph Laplacian [24]. To simulate the wave dynamics discretely, we discretize the wave equation on a graph into

$$\mathbf{u}_i(t) = 2\mathbf{u}_i(t-1) - \mathbf{u}_i(t-2) - c^2 \sum_{j \in \mathcal{N}(i)} \mathbf{L}_{ij}\mathbf{u}_j(t-1), \quad (21)$$

where \mathbf{u}_i is the i -th element of \mathbf{u} . [23] simulated the wave dynamics with $dt = 1$ on a digital computer. As this simulation only involves matrix-vector multiplication, we can replace this $\mathcal{O}(N^2)$ operation on digital computers with $\mathcal{O}(1)$ operation on analog computers or $\mathcal{O}(N)$ on quantum computers [31, 15].

Simulating wave dynamics on a graph this way has a time complexity of $\mathcal{O}(D^{5/2}l/a + TD^2/a)$, where T is the terminal time of simulation, D is the dimension of the wave, l is the diameter of the region, and a is the step size [32]. For our case, the dimension D is 2 (time and space), the diameter of the region l is the number of nodes N , and the step size a is 1, so the complexity is $\mathcal{O}(N + T)$. In practice, we simulate the wave dynamics for around $2N$, leading to an $\mathcal{O}(N)$ computational complexity. As $T = 2N$ leads to large simulation times for big systems, we can no longer ignore the approximation errors from the discrete system, and an errorless continuous simulation is favorable.

To continuously simulate the wave dynamics and avoid truncation errors, [32] suggests simulating on quantum computers with Hamiltonian simulation and quantum linear system algorithms. Quantum computers process the following Hamiltonian system

$$\frac{d\mathbf{u}}{dt} = -i\mathbf{H}\mathbf{u}(t), \quad (22)$$

for a certain time before making measurements, where \mathbf{H} is the Hermitian static Hamiltonian [28].

Consider the case where \mathbf{L} is the symmetric normalized graph Laplacian. We have $\mathbf{L} = \mathbf{B}\mathbf{B}^T$, where \mathbf{B} is the signed incidence matrix of the graph. For a graph with N nodes and M edges, the $N \times M$ incidence matrix \mathbf{B} has rows indexed by nodes v and columns indexed by edges e (connecting nodes i and j), defined as

$$\mathbf{B}_{ij} = \begin{cases} -1 & \text{if edge } e_j \text{ leaves vertex } v_i, \\ 1 & \text{if edge } e_j \text{ enters vertex } v_i, \\ 0 & \text{otherwise.} \end{cases}$$

Define a Hermitian Hamiltonian in the following block form

$$H = c \begin{bmatrix} \mathbf{0} & \mathbf{B} \\ \mathbf{B} & \mathbf{0} \end{bmatrix}. \quad (23)$$

The Schrödinger Hamiltonian system takes the form

$$\frac{d}{dt} \begin{bmatrix} \mathbf{u}_1 \\ \mathbf{u}_2 \end{bmatrix} = -ic \begin{bmatrix} \mathbf{0} & \mathbf{B} \\ \mathbf{B} & \mathbf{0} \end{bmatrix} \begin{bmatrix} \mathbf{u}_1 \\ \mathbf{u}_2 \end{bmatrix}, \quad (24)$$

which implies

$$\frac{d^2}{dt^2} \begin{bmatrix} \mathbf{u}_1 \\ \mathbf{u}_2 \end{bmatrix} = -c^2 \begin{bmatrix} \mathbf{0} & \mathbf{B} \\ \mathbf{B} & \mathbf{0} \end{bmatrix}^2 \begin{bmatrix} \mathbf{u}_1 \\ \mathbf{u}_2 \end{bmatrix} = -c^2 \begin{bmatrix} \mathbf{B}\mathbf{B}^T & \mathbf{0} \\ \mathbf{0} & \mathbf{B}^T\mathbf{B} \end{bmatrix} \begin{bmatrix} \mathbf{u}_1 \\ \mathbf{u}_2 \end{bmatrix} = -c^2 \begin{bmatrix} L & \mathbf{0} \\ \mathbf{0} & \mathbf{B}^T\mathbf{B} \end{bmatrix} \begin{bmatrix} \mathbf{u}_1 \\ \mathbf{u}_2 \end{bmatrix} [32]. \quad (25)$$

In simulating dynamics with the Schrödinger system 25, the first N terms correspond to wave dynamics. When \mathbf{u} has a non-zero initial derivative condition, the resulting solution tends to increase over time, leading to instability [33]. This is evident given that:

$$\frac{d}{dt} \begin{bmatrix} \mathbf{u}_1 \\ \mathbf{u}_2 \end{bmatrix} = -ic \begin{bmatrix} \mathbf{0} & \mathbf{B} \\ \mathbf{B} & \mathbf{0} \end{bmatrix} \begin{bmatrix} \mathbf{u}_1 \\ \mathbf{u}_2 \end{bmatrix} = -ic \begin{bmatrix} \mathbf{B}\mathbf{u}_2 \\ \mathbf{B}\mathbf{u}_1 \end{bmatrix}, \quad (26)$$

$\frac{d\mathbf{u}_1}{dt}(0) = \mathbf{0}$ translates to the initial condition $\mathbf{u}_1(0) = \mathbf{0}$.

The graph Laplacian used in [22, 23] is the random-walk graph Laplacian L_{rw} . However, since this is not Hermitian, the wave dynamics based on L_{rw} cannot be simulated with quantum computers. We instead investigate using the symmetric graph Laplacian L_{sym} , defined as

$$\mathbf{L}_{sym} = \mathbf{I} - \mathbf{D}^{-1/2}\mathbf{W}\mathbf{D}^{1/2}, \quad (27)$$

where $D = \text{diag}(\sum_{j=1}^n \mathbf{W}_{1j}, \sum_{j=1}^n \mathbf{W}_{2j}, \dots, \sum_{j=1}^n \mathbf{W}_{nj})$. To validate that the wave dynamics simulated on a quantum computer is stable, we prove that the wave dynamics with L_{sym} is stable under the same conditions as L_{rw} :

Lemma 3. *The wave equation iteration 26 is stable on any graph if the wave speed c satisfies $0 < c < \sqrt{2}$, with an initial condition of $\mathbf{u}_1(-1) = \mathbf{u}_1(0)$.*

Proof. We have the dynamics of $z(t) = [u(t); u(t-1)]$ evolves as

$$z(t) = \begin{bmatrix} u(t) \\ u(t-1) \end{bmatrix} = \begin{bmatrix} 2I - c^2 L_{sym} & -I \\ I & 0 \end{bmatrix} \begin{bmatrix} u(t-1) \\ u(t-2) \end{bmatrix} = Mz(t-1) = M^t z(0).$$

Denote M 's eigen-vector as $(a_j, b_j)^T$, and M 's eigenvalue as α_j . Since we know

$$M \begin{bmatrix} a_j \\ b_j \end{bmatrix} = \begin{bmatrix} 2I - c^2 L_{sym} & -I \\ I & 0 \end{bmatrix} \begin{bmatrix} a_j \\ b_j \end{bmatrix} = \begin{bmatrix} 2a_j - c^2 L a_j - b_j \\ a_j \end{bmatrix}, \text{ and } M \begin{bmatrix} a_j \\ b_j \end{bmatrix} = \alpha_j \begin{bmatrix} a_j \\ b_j \end{bmatrix} = \begin{bmatrix} \alpha_j a_j \\ \alpha_j b_j \end{bmatrix}.$$

If we denote $b_j = v_j$, we have $a_j = \alpha_j b_j = \alpha_j v_j$, and have the eigenvector m_j of M is $m_j = (\alpha_j v_j, v_j)^T$.

By the definition of eigenvalues,

$$M \begin{bmatrix} \alpha_j v_j \\ v_j \end{bmatrix} = \alpha_j \begin{bmatrix} \alpha_j v_j \\ v_j \end{bmatrix} \Rightarrow \begin{bmatrix} (\alpha_j(2 - \alpha_j)I - \alpha_j c^2 L_{sym} - I)v_j \\ 0 \end{bmatrix} = \begin{bmatrix} 0 \\ 0 \end{bmatrix}.$$

Denote the eigenvalue of L_{sym} as λ_j , we have

$$\alpha_j(2 - \alpha_j)v_j - c^2 \alpha_j L_{sym} v_j - v_j = 0 \Rightarrow \alpha_j^2 + (c^2 \lambda_j - 2)\alpha_j + 1 = 0,$$

so we have

$$\alpha_j = \frac{-(c^2 \lambda_j - 2) \pm \sqrt{(c^2 \lambda_j - 2)^2 - 4}}{2} = \frac{2 - c^2 \lambda_j}{2} \pm \frac{c}{2} \sqrt{c^2 \lambda_j^2 - 4\lambda_j}$$

Therefore, to generate stable dynamics with M , we need L_{sym} 's eigenvalues λ_j 's to satisfy $c^2 \lambda_j^2 - 4\lambda_j < 0$, resulting in $\lambda_j \in (0, \sqrt{2})$. □

3.4 Eigendecomposition with analog computers

To calculate the eigenvalues and eigenvector components at node l using DMD, we begin with a reduced SVD in matrix \mathbf{X} . Despite existing quantum methods' superior polylog complexity for SVDs, they work on low-rank matrices, which is not the case here [34]. We instead focus on efficient methods performed on analog computers. It's important to note that the eigenvalues of $\mathbf{X}^T \mathbf{X}$, represented as $\sqrt{\gamma_i}$, correspond to the squared singular values of \mathbf{X} [35]. Since $\mathbf{X}^T \mathbf{X}$ is symmetric, it has distinct real eigenvalues, which can be determined using the power method.

The power method approximates dominant eigenvalues (and their corresponding eigenvectors) of matrices. Especially powerful for large-scale matrices, this method iteratively refines estimates of the dominant eigenvector, capitalizing on the property that repeated multiplication accentuates the contribution of the dominant eigenvalue. The following recurrence relation describes the power method:

$$\mathbf{b}_{k+1} = \frac{\mathbf{X}^T \mathbf{X} \mathbf{b}_k}{\|\mathbf{X}^T \mathbf{X} \mathbf{b}_k\|}. \quad (28)$$

Using the eigenvector \mathbf{b}_k , the estimation for the dominant eigenvalue is the Rayleigh quotient

$$\gamma_k = \frac{\mathbf{b}_k^T \mathbf{X}^T \mathbf{X} \mathbf{b}_k}{\mathbf{b}_k^T \mathbf{b}_k} [35]. \quad (29)$$

To calculate other eigenvalues and eigenvectors using the power method, we need to remove the dominant eigenvalue while preserving the spectrum. Deflation methods such as Wielandt's and Hotelling's deflation provide such tools [36, 37]. Hotelling's deflation states that

Lemma 4. *If $\gamma_1 \geq \gamma_2 \geq \dots \geq \gamma_N$ are the eigenvalues of \mathbf{A} , $\mathbf{b}^{(1)}, \mathbf{b}^{(2)}, \dots, \mathbf{b}^{(N)}$ are the corresponding eigenvectors. Then $\hat{\mathbf{A}} = \mathbf{A} - \mathbf{b}^{(j)} \mathbf{b}^{(j)T} \mathbf{A} \mathbf{b}^{(j)} \mathbf{b}^{(j)T}$ for some $j \in \{1, 2, \dots, N\}$. Then $\hat{\mathbf{A}}$ has eigenvectors $\mathbf{b}^{(1)}, \mathbf{b}^{(2)}, \dots, \mathbf{b}^{(N)}$ with corresponding eigenvalues $\gamma_1, \dots, \gamma_{j-1}, 0, \gamma_{j+1}, \dots, \gamma_N$ [37].*

Hotelling’s deflation maintains the full spectrum of a matrix, nullifying a chosen eigenvalue while keeping the rest intact. Implementation of Hotelling’s deflation is straightforward with just matrix-vector multiplications. Due to the approximation error inherent in the power method, Hotelling’s deflation does not eliminate the eigenvalues, causing numerical instabilities for higher-dimensional matrices. Schur’s deflation method improves this issue, which remains stable despite the uneliminated eigenvalues and converges back to Hotelling’s deflation when the elimination is exact [37]. Consequently, the power method struggles to determine smaller eigenvalues. Since we employ a reduced SVD, disregarding exceedingly small singular values, this numerical challenge does not affect the efficiency of our algorithm [35].

Define the SVD of \mathbf{X} as $\mathbf{X} = \mathbf{U}\mathbf{\Sigma}\mathbf{V}^T$. The eigendecomposition with the power method and Hotelling’s deflation provides us the singular values of \mathbf{X} , which form the diagonal of $\mathbf{\Sigma}$, as well as the eigenvectors of $\mathbf{X}^T\mathbf{X}$, which are the columns of \mathbf{V} . When performing a reduced SVD, we keep only $M \ll N$ singular values and columns of \mathbf{V} . We can calculate \mathbf{U} with a pseudoinverse of $\mathbf{V}_{\text{red}}^T$ given by

$$\mathbf{U}_{\text{red}} \approx \mathbf{X}\mathbf{V}_{\text{red}}^{T+}\mathbf{\Sigma}_{\text{red}}^{-1}, \tag{30}$$

where $\mathbf{V}_{\text{red}}^{T+}$ is the pseudoinverse of $\mathbf{V}_{\text{red}}^T$. Both quantum computers and analog computers provide efficient methods of computing pseudoinverse [38, 15].

The subsequent phase of DMD involves calculating the eigenvalues of $\tilde{\mathbf{A}} = \mathbf{U}^*\mathbf{Y}\mathbf{V}\mathbf{\Sigma}^{-1}$. The power method isn’t applicable on unsymmetric matrix $\tilde{\mathbf{A}}$. However, given that $\tilde{\mathbf{A}}$ is of dimensions $\mathbb{R}^{M \times M}$ and $M \ll N$, standard eigendecomposition techniques are not heavily impacted by the large dimensionality N . Analog computers provide an $\mathcal{O}(M \log M)$ complexity, which arises from the M linear system solves. Quantum algorithms provide the same scaling. However, existing algorithms assume properties on the matrix, such as Hermitian, diagonalizable, etc. [39, 40, 41]

3.5 Solving linear systems with quantum computers

The last step of DMD is to solve the linear system $\hat{\Phi}\hat{\mathbf{a}} = \mathbf{x}(0)$. Quantum computers excel at this task, with time complexity of $\mathcal{O}(\text{poly}(\log N, \kappa))$, where N and κ are the dimension and condition number of $\hat{\Phi}$, whereas classical algorithms in $\mathcal{O}(N\sqrt{\kappa})$ time [13].

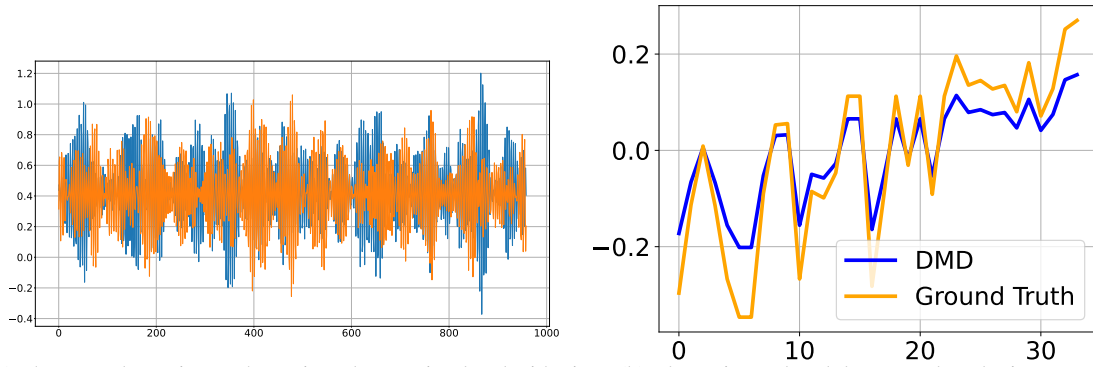
	Digital	Analog	Quantum
Simulate Wave Dynamics	$\mathcal{O}(N^2N_t)$	$\mathcal{O}(N_t)$	$\mathcal{O}(N)$
Reduced SVD	$\mathcal{O}(M^2N + M^3)$	$\mathcal{O}(KM)$	$\mathcal{O}(\text{poly } \log N)$
Eigendecomposition	$\mathcal{O}(M^3)$	$\mathcal{O}(M \log M)$	$\mathcal{O}(M \log M)^*$
Matrix-vector multiplication	$\mathcal{O}(N^2)$	$\mathcal{O}(1)$	$\mathcal{O}(N)$
Solving linear system	$\mathcal{O}(N^3)$	$\mathcal{O}(\log N)$	$\mathcal{O}(\log N)$

Table 1: Computational complexities of operations involved. H is the Hermitian static Hamiltonian, N is the number of nodes, N_t is the number of time steps, K is the number of iterations taken for the power method, M is the number of components left in reduced SVD, T is terminal time [42, 15, 13]. Although we listed the complexity of quantum matrix-vector multiplication, there are no quantum matrix-vector multiplication algorithms and only quantum matrix multiplication algorithms, with an $\mathcal{O}(N^2)$ complexity [43].

4 Result

We performed numerical experiments on the proposed method to verify that its results match those of classical algorithms. First, as shown in Figure 2b, we experiment with a benchmark called Zachary’s karate club graph [44]. Zachary’s Karate Club graph is a widely studied social network representing the relationships between a karate club’s 34 members at a US university in the 1970s. In the graph, each node represents a member of the karate club, and each edge between two nodes indicates a tie between two members outside of the club activities. The network is undirected and unweighted, reflecting the mutual nature of social relationships. We simulated the wave dynamics on Qiskit dynamics from time $t = 0$ to $t = 99$, measuring the dynamics at integer times [45]. As expected, the eigenvector estimated by the proposed method is a constant time of the ground truth. Since the ground truth eigenvector and the prediction share the same parity, which is used to assign clusters, the estimated clusters perfectly match.

We also demonstrate the performance of our method on the Twitter interaction network for the US Congress, which represents the Twitter interaction network of both the House of Representatives and Senate at the 117th United States Congress [46, 47]. As shown in Figure 3, our method classifies 467 out of 475 nodes right, which equals an accuracy of

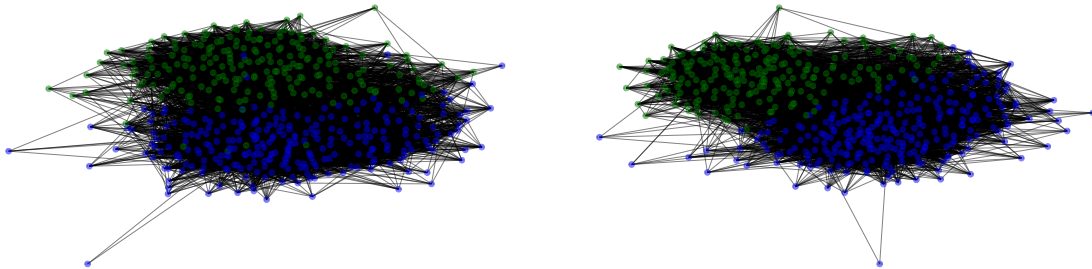


(a) The wave dynamics on the Twitter dataset simulated with qiskit dynamics verifies the stability of quantum-simulated dynamics. (b) The estimated and the ground truth eigenvector of the adjacency matrix of the Karate club network.

Figure 2: The ground truth eigenvector and ten times of the eigenvector calculated with proposed method. We calculate the clusters with the signs of the eigenvector.

98.32%. This error comes from the numerical errors of simulating the quantum dynamics on Qiskit dynamics, rather than using an actual quantum computer, and from the deflation method of the power method.

To verify the stability of the wave equation simulated with the L_{symm} , we additionally plot the wave dynamics used for clustering the Twitter dataset.



(a) The clusters calculated according to the eigenvector estimated with the proposed method. (b) Ground Truth cluster calculated with spectral clustering.

Figure 3: Clusters of the Twitter interaction network for the US congress, comparing the ground truth and the ones calculated with proposed method.

Lastly, we test the proposed method on a synthetic network with eighty nodes and four clusters. The network contains four clusters of nodes, where the nodes in each cluster are closely connected, and the four clusters connect loosely. As shown in figure 4, our method perfectly estimates the clusters.

5 Conclusion

We propose a first-of-a-kind quantum-analog hybrid algorithm to cluster large-scale graphs. The algorithm contains two components that are used sequentially. In the first component, we simulate wave dynamics on a graph on analog (discretized dynamics) or quantum (continuous dynamics) computers. Both analog and quantum platforms accelerate the computations by a polynomial factor. However, fault tolerant quantum computers are expected to provide a major advantage over analog computers for the simulation of wave dynamics, due to its inherent lack of discretization error, thereby resulting in robustness for large graphs. In the second component, where we analyze the data from the wave dynamics using dynamic mode decomposition on analog platforms. In this step, we achieve polynomial speedups over digital computers, arising from the $\mathcal{O}(1)$ complexity of matrix-vector multiplication on analog platforms. Overall, we accelerate the previous $\mathcal{O}(N^3)$ complexity on digital computers to $\mathcal{O}(N)$ on the quantum-analog hybrid platform. We

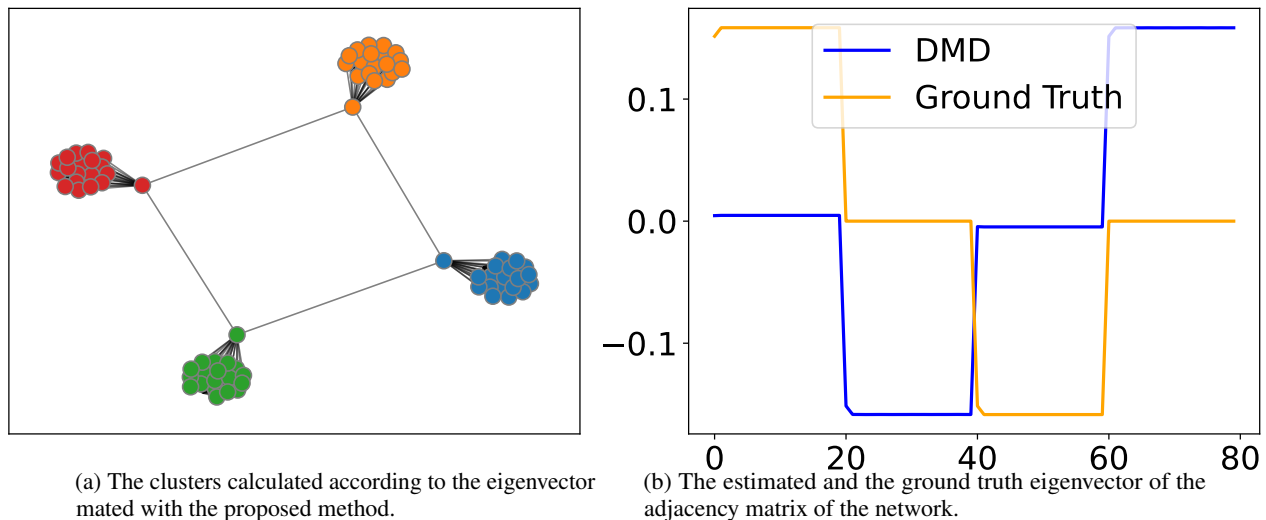


Figure 4: Estimated clusters of the synthetic network and the comparison of the estimated and ground truth eigenvector.

demonstrate the proposed algorithm on various benchmark datasets including the Zachary Karate club example, Twitter interaction networks, and random graphs.

In the broader picture, this work demonstrates that embeddings of discrete problems in continuous spaces enables the construction of efficient algorithms on emerging computing devices. Moreover, we expect that novel combinations of digital, analog, and quantum platforms provide a unique opportunity for the development of novel and efficient algorithms that exploit the inherent strength of each platform. As these computing platforms mature, we expect an increase in the development of such algorithms that exploit the dynamical nature of these problems and devices. We also note, that these embeddings provide deep insights into the fundamental limitations of algorithm construction and related complexity classes [48] and remains an underexplored area of research.

References

- [1] Nina Mishra, Robert Schreiber, Isabelle Stanton, and Robert E Tarjan. Clustering social networks. In *International Workshop on Algorithms and Models for the Web-Graph*, pages 56–67, New York, NY, 2007. Springer.
- [2] Ruifang Liu, Shan Feng, Ruisheng Shi, and Wenbin Guo. Weighted graph clustering for community detection of large social networks. *Procedia Computer Science*, 31:85–94, 2014.
- [3] Zhan Bu, Jie Cao, Hui-Jia Li, Guangliang Gao, and Haicheng Tao. Gleam: A graph clustering framework based on potential game optimization for large-scale social networks. *Knowledge and Information Systems*, 55:741–770, 2018.
- [4] Andrei Sorin Sabau. Survey of clustering based financial fraud detection research. *Informatica Economica*, 16(1):110, 2012.
- [5] Tahereh Pourhabibi, Kok-Leong Ong, Booi H Kam, and Yee Ling Boo. Fraud detection: A systematic literature review of graph-based anomaly detection approaches. *Decision Support Systems*, 133:113303, 2020.
- [6] Desmond J Higham, Gabriela Kalna, and Milla Kibble. Spectral clustering and its use in bioinformatics. *Journal of computational and applied mathematics*, 204(1):25–37, 2007.
- [7] Amit Surana, Tuhin Sahai, and Andrzej Banaszuk. Iterative methods for scalable uncertainty quantification in complex networks. *International Journal for Uncertainty Quantification*, 2(4):413–439, 2012.
- [8] Stefan Klus, Tuhin Sahai, Cong Liu, and Michael Dellnitz. An efficient algorithm for the parallel solution of high-dimensional differential equations. *Journal of computational and applied mathematics*, 235(9):3053–3062, 2011.
- [9] Shabbir Ahmed and Salil S Kanhere. Cluster-based forwarding in delay tolerant public transport networks. In *32nd IEEE Conference on Local Computer Networks (LCN 2007)*, pages 625–634, Piscataway, NJ, 2007. IEEE.

- [10] Ulrike Von Luxburg. A tutorial on spectral clustering. *Statistics and computing*, 17:395–416, 2007.
- [11] Peter W Shor. Polynomial-time algorithms for prime factorization and discrete logarithms on a quantum computer. *SIAM review*, 41(2):303–332, 1999.
- [12] Lov K Grover. A fast quantum mechanical algorithm for database search. In *Proceedings of the twenty-eighth annual ACM symposium on Theory of computing*, pages 212–219, 1601 Broadway, 10th Floor, New York, NY, 1996. ACM.
- [13] Aram W. Harrow, Avinatan Hassidim, and Seth Lloyd. Quantum algorithm for linear systems of equations. *Phys. Rev. Lett.*, 103:150502, Oct 2009.
- [14] Hong Li, Nan Jiang, Zichen Wang, Jian Wang, and Rigui Zhou. Quantum matrix multiplier. *International Journal of Theoretical Physics*, 60:2037–2048, 2021.
- [15] Zhong Sun and Daniele Ielmini. Invited tutorial: Analog matrix computing with crosspoint resistive memory arrays. *IEEE Transactions on Circuits and Systems II: Express Briefs*, 69(7):3024–3029, 2022.
- [16] Zhong Sun, Giacomo Pedretti, Piergiulio Mannocci, Elia Ambrosi, Alessandro Bricalli, and Daniele Ielmini. Time complexity of in-memory solution of linear systems. *IEEE Transactions on Electron Devices*, 67(7):2945–2951, 2020.
- [17] Scott White and Pádraic Smyth. *A Spectral Clustering Approach To Finding Communities in Graphs*, pages 274–285. Society for Industrial and Applied Mathematics, Department of Computer Science Donald Bren School of Information and Computer Sciences University of California, Irvine 3019 Donald Bren Hall Irvine, CA 92697-3435, 2005.
- [18] R.R. Schaller. Moore’s law: past, present and future. *IEEE Spectrum*, 34(6):52–59, 1997.
- [19] James R. Powell. The quantum limit to moore’s law. *Proceedings of the IEEE*, 96(8):1247–1248, 2008.
- [20] Edward T. Gilbert-Kawai and Marc D. Wittenberg. *Ohm’s law, voltage, current and resistance*. Cambridge University Press, 1 Liberty Plaza New York, NY 10006, 2014.
- [21] Zhong Sun and Ru Huang. Time complexity of in-memory matrix-vector multiplication. *IEEE Transactions on Circuits and Systems II: Express Briefs*, 68(8):2785–2789, 2021.
- [22] Tuhin Sahai, Alberto Speranzon, and Andrzej Banaszuk. Hearing the clusters of a graph: A distributed algorithm. *Automatica*, 48(1):15–24, 2012.
- [23] Hongyu Zhu, Stefan Klus, and Tuhin Sahai. A dynamic mode decomposition approach for decentralized spectral clustering of graphs. In *2022 IEEE Conference on Control Technology and Applications (CCTA)*, pages 1202–1207, IEEE Operations Center, 445 Hoes Lane, Piscataway, NJ 08854, 2022. IEEE, IEEE Conference on Control Technology and Applications.
- [24] Joel Friedman and Jean-Pierre Tillich. Wave equations for graphs and the edge-based laplacian. *Pacific Journal of Mathematics*, 216:229–266, 2004.
- [25] Jonathan Tu, Clarence Rowley, Dirk Luchtenburg, Steven Brunton, and Nathan Kutz. On dynamic mode decomposition: Theory and applications. *ACM Journal of Computer Documentation*, 1:391–421, 2013.
- [26] Daniel Dylewsky, Eurika Kaiser, Steven L. Brunton, and J. Nathan Kutz. Principal component trajectories for modeling spectrally-continuous dynamics as forced linear systems, 2022.
- [27] Virginia Vassilevska Williams, Yinzhan Xu, Zixuan Xu, and Renfei Zhou. New bounds for matrix multiplication: from alpha to omega. *ArXiv*, abs/2307.07970, 2023.
- [28] Luca Tagliacozzo. Optimal simulation of quantum dynamics. *Nature Physics*, 18(9):970–971, 2022.
- [29] Abeynaya Gnanasekaran, Amit Surana, and Tuhin Sahai. Efficient quantum algorithms for nonlinear stochastic dynamical systems. In *2023 IEEE International Conference on Quantum Computing and Engineering (QCE)*, volume 2, pages 66–75, Bellevue, WA, USA, 2023. IEEE, 2023 IEEE International Conference on Quantum Computing and Engineering.
- [30] Amit Surana, Abeynaya Gnanasekaran, and Tuhin Sahai. An efficient quantum algorithm for simulating polynomial dynamical systems. *Quantum Information Processing*, 23(3):105, 2024.
- [31] Xin-Ding Zhang, Xiao-Ming Zhang, and Zheng-Yuan Xue. Quantum hyperparallel algorithm for matrix multiplication. *Scientific Reports*, 6:24910, 2016.
- [32] Pedro C. S. Costa, Stephen Jordan, and Aaron Ostrander. Quantum algorithm for simulating the wave equation. *Phys. Rev. A*, 99:012323, Jan 2019.

- [33] Lawrence C Evans. *Partial differential equations*, volume 19. American Mathematical Society, Ann Arbor, Michigan, 2022.
- [34] Patrick Reberntrost, Adrian Steffens, Iman Marvian, and Seth Lloyd. Quantum singular-value decomposition of nonsparse low-rank matrices. *Phys. Rev. A*, 97:012327, Jan 2018.
- [35] Martin Anthony and Michele Harvey. *Advanced linear algebra*. Springer, Hanover, Pennsylvania, 2006.
- [36] Yousef Saad. *Numerical Methods for Large Eigenvalue Problems: Revised Edition*. SIAM, Philadelphia, Pennsylvania, 2011.
- [37] Lester Mackey. Deflation methods for sparse pca. In D. Koller, D. Schuurmans, Y. Bengio, and L. Bottou, editors, *Advances in Neural Information Processing Systems*, volume 21, Vancouver, British Columbia, 2008. Curran Associates, Inc.
- [38] Nathan Wiebe, Daniel Braun, and Seth Lloyd. Quantum algorithm for data fitting. *Phys. Rev. Lett.*, 109:050505, Aug 2012.
- [39] Nhat A. Nghiem and Tzu-Chieh Wei. Quantum algorithm for estimating largest eigenvalues. *Physics Letters A*, 488:129138, November 2023.
- [40] Changpeng Shao. Computing eigenvalues of diagonalizable matrices on a quantum computer. *ACM Transactions on Quantum Computing*, 3(4), jul 2022.
- [41] Seth Lloyd, Masoud Mohseni, and Patrick Reberntrost. Quantum principal component analysis. *Nature Physics*, 10(9):631–633, 2014.
- [42] Xiaocan Li, Shuo Wang, and Yinghao Cai. Tutorial: Complexity analysis of singular value decomposition and its variants, 2019.
- [43] Changpeng Shao. Quantum algorithms to matrix multiplication, 2018.
- [44] M. Girvan and M. E. J. Newman. Community structure in social and biological networks. *Proceedings of the National Academy of Sciences*, 99(12):7821–7826, June 2002.
- [45] Daniel Puzzuoli, Christopher J. Wood, Daniel J. Egger, Benjamin Rosand, and Kento Ueda. Qiskit Dynamics: A Python package for simulating the time dynamics of quantum systems. *Journal of Open Source Software*, 8(90):5853, 2023.
- [46] Christian G Fink, Nathan Omodt, Sydney Zinnecker, and Gina Sprint. A congressional twitter network dataset quantifying pairwise probability of influence. *Data in Brief*, 50:109521, 2023.
- [47] Christian G Fink, Kelly Fullin, Guillermo Gutierrez, Nathan Omodt, Sydney Zinnecker, Gina Sprint, and Sean McCulloch. A centrality measure for quantifying spread on weighted, directed networks. *Physica A*, 626:129083, 2023.
- [48] Tuhin Sahai and Abeynaya Gnanasekaran. On the emergence of ergodic dynamics in unique games, 2024.